


Analytical solutions for quantum radiation reaction in high-intensity lasers

T. G. Blackburn ^{*}

Department of Physics, University of Gothenburg, SE-41296 Gothenburg, Sweden

 (Received 3 January 2024; accepted 6 February 2024; published 23 February 2024)

While the Landau-Lifshitz equation, which describes classical radiation reaction, can be solved exactly and analytically for a charged particle accelerated by a plane electromagnetic wave, no such solutions are available for quantum radiation reaction (the recoil arising from the successive, incoherent emission of hard photons). Yet upcoming experiments with ultrarelativistic electron beams and high-intensity lasers will explore the regime where both radiation-reaction and quantum effects are important. Here we present analytical solutions for the mean and variance of the energy distribution of an electron beam that collides with a pulsed plane electromagnetic wave, which are obtained by means of a perturbative expansion in the quantum parameter χ_0 . These solutions capture both the quantum reduction in the radiated power and the stochastic broadening, and are shown to be accurate across the range of experimentally relevant collision parameters, i.e., GeV-class electron beams and laser amplitudes $a_0 \lesssim 200$.

DOI: [10.1103/PhysRevA.109.022234](https://doi.org/10.1103/PhysRevA.109.022234)

I. INTRODUCTION

The electromagnetic fields produced by focused high-power lasers are so strong that the dynamics of relativistic particles enters the regime of strong-field QED [1–3]. One process that has attracted much interest is quantum radiation reaction, i.e., the accumulated recoil from the emission of individual high-energy photons [4], which can be as significant to the particle and plasma dynamics as the acceleration induced by the background electromagnetic field [2]. Experiments with high-intensity lasers have already shown evidence of radiation reaction [5,6], and investigation of strong-field QED effects, including quantum radiation reaction, is a key part of the science case for upcoming and planned laser facilities [7–12].

Quantum radiation reaction has many possible experimental signatures, including stochastic broadening [13], straggling [14], quenching [15], and increased angular divergence [16,17], all of which arise because photon emission is inherently probabilistic. These works rely largely on the results of numerical simulations, as the theory for quantum radiation reaction is not generally amenable to analytical solution. By contrast, the Landau-Lifshitz equation [18], which describes classical radiation reaction, can be solved exactly for a general plane-wave background [19] (see also Refs. [20–22]). It would be helpful for guidance of future experiments to have analytical solutions that apply in the quantum regime. In this work we consider the radiation reaction of an ultrarelativistic electron beam in an intense laser

background, but note that similar phenomena can be explored with aligned crystals [23–26].

Consider a beam of ultrarelativistic electrons, which has a distribution of Lorentz factors γ , $\frac{dN_\gamma}{d\gamma}$, characterized by a mean $\mu = \langle \gamma \rangle$, variance $\sigma^2 = \langle (\gamma - \mu)^2 \rangle$, and other higher-order moments including $\zeta^3 = \langle (\gamma - \mu)^3 \rangle$ and $\kappa^4 = \langle (\gamma - \mu)^4 \rangle$, which are related to the skewness and kurtosis, respectively. This beam collides with an intense laser pulse, which is modeled as a plane electromagnetic wave with angular frequency ω_0 and normalized amplitude a_0 , such that the electric field as a function of phase ϕ is $\mathbf{E}(\phi) = m\omega_0 a_0 \mathbf{f}(\phi)/e$. Here e and m are the elementary charge and the electron mass, respectively, and we work in natural units where $\hbar = c = 1$. As the electron beam propagates through the laser pulse, it emits radiation and decelerates.

If the electrons are ultrarelativistic, radiation emission and reaction may be treated within the semiclassical framework proposed by Baier and Katkov [27]. Provided that $\gamma \gg a_0$ and a_0 is large enough that the locally constant field approximation holds [28–31], the evolution of the mean and variance of the energy distribution is given by [32,33]

$$\frac{d\mu}{d\phi} = -\frac{2R_c}{3\mu_0} |f(\phi)|^2 \langle \gamma^2 g(\chi) \rangle, \quad (1)$$

and

$$\begin{aligned} \frac{d\sigma^2}{d\phi} = & -\frac{4R_c}{3\mu_0} |f(\phi)|^2 \langle (\gamma - \mu) \gamma^2 g(\chi) \rangle \\ & + \frac{55R_c \chi_0}{24\sqrt{3}\mu_0^2} |f(\phi)|^3 \langle \gamma^4 g_2(\chi) \rangle, \end{aligned} \quad (2)$$

where $R_c = \alpha a_0 \chi_0$ is the classical radiation reaction parameter, $\chi_0 = 2a_0 \mu_0 \omega_0 / m$ is the quantum parameter, and μ_0 is the initial value of the mean. The unsubscripted χ appearing in these equations is the instantaneous value of the quantum parameter $\chi = 2a_0 \gamma \omega_0 |f(\phi)| / m$, which depends on the instantaneous γ and field amplitude. The two functions $g(\chi)$

^{*}tom.blackburn@physics.gu.se

Published by the American Physical Society under the terms of the Creative Commons Attribution 4.0 International license. Further distribution of this work must maintain attribution to the author(s) and the published article's title, journal citation, and DOI. Funded by Bibsam.

and $g_2(\chi)$ describe the role of quantum corrections to radiation reaction and are discussed in Sec. II.

The purpose of this work is to find analytical predictions of the mean and variance in the regime where quantum effects are important, but not dominant. Equivalent results for the classical regime $\chi_0 = 0$ have been obtained by Neitz and Di Piazza [13] and Vranic *et al.* [17,34]. This analysis is extended to the quantum regime and to the whole hierarchy of moments by Niel *et al.* [33]. The dynamics of the energy distribution itself, rather than its moments, under quantum radiation reaction is treated analytically in Bulanov *et al.* [35]. Furthermore, the evolution of the mean and variance in a constant field has been obtained by Torgrimsson [36,37], using a resummation approach. The strategy here is to solve Eqs. (1) and (2) perturbatively in the small parameter χ_0 . Additionally, to break the infinite hierarchy that arises because the evolution of a given moment depends on higher-order moments, we make the approximation that successive moments are smaller than each other, i.e., $\mu \gg \sigma \gg \kappa$. We begin by discussing the functions $g(\chi)$ and $g_2(\chi)$, and then we present analytical solutions for the mean and variance of the distribution.

II. QUANTUM CORRECTIONS

Quantum effects are manifest in the two functions $g(\chi)$ and $g_2(\chi)$, which relate moments of the quantum and classical synchrotron emissivities. In particular, $g(\chi)$ represents the reduction in the radiation power caused by quantum corrections to the synchrotron spectrum.

We define the n th moment of the radiation spectrum to be

$$\mathcal{M}(n, \chi) = \int (\chi s)^n \frac{dW_\gamma}{ds} ds, \quad (3)$$

$$\tilde{\mathcal{M}}(n, \chi) = \frac{2}{\Gamma(\frac{n}{2} + \frac{1}{6})\Gamma(\frac{n}{2} + \frac{11}{6})} \int_0^\infty \left[\frac{(n+1)y^n (8 + 12\chi y + 9\chi^2 y^2) K_{2/3}(y)}{(2 + 3\chi y)^{n+3}} - \frac{y^{n+1} K_{1/3}(y)}{(2 + 3\chi y)^{n+1}} \right] dy, \quad (7)$$

which can be evaluated numerically for any n and χ . Limiting values of Eq. (7) are, for $\chi \ll 1$,

$$\tilde{\mathcal{M}}(n, \chi) = 1 - \frac{3(n+1)\Gamma(\frac{n}{2} + \frac{2}{3})\Gamma(\frac{n}{2} + \frac{7}{3})}{\Gamma(\frac{n}{2} + \frac{1}{6})\Gamma(\frac{n}{2} + \frac{11}{6})} \chi + \frac{(n+1)(3n+1)[28 + n(3n+17)]}{8} \chi^2 + \dots, \quad (8)$$

and, for $\chi \gg 1$,

$$\tilde{\mathcal{M}}(n, \chi) = -\frac{(n+1)[28 + 9n(n+3)]\Gamma(-\frac{1}{3})\Gamma(\frac{2}{3})\Gamma(n + \frac{1}{3})}{27\Gamma(\frac{n}{2} + \frac{1}{6})\Gamma(\frac{n}{2} + \frac{11}{6})\Gamma(n+3)} (3\chi)^{-n-1/3}. \quad (9)$$

Examples of moments at specific orders are given in Table I.

III. MEAN ENERGY LOSS

We begin by expanding Eq. (1) to first order in χ_0 . This requires $g(\chi)$ to first order in χ , which is given in Table I:

$$\frac{d\hat{\mu}}{d\phi} = -\frac{2}{3} R_c |f(\phi)|^2 \hat{\mu}^2 \left[\left(1 + \frac{\sigma^2}{\mu^2} \right) - \frac{55\sqrt{3}}{16} \chi_0 |f(\phi)| \hat{\mu} \left(1 + \frac{3\sigma^2}{\mu^2} + \frac{\zeta^3}{\mu^3} \right) \right], \quad (10)$$

where $\hat{\mu} = \mu/\mu_0$ is the mean energy normalized to its initial value. The expansion in Eq. (10) is effectively an expansion to first order in \hbar , even though we work in natural units,

where $\frac{dW_\gamma}{ds}$ is the photon emission rate per unit proper time, per unit photon normalized energy $s = \omega'/(\gamma m)$, as calculated in the locally constant field approximation [28,38]:

$$\frac{dW_\gamma}{ds} = \frac{\alpha m}{\sqrt{3}\pi} \left[\left(1 - s + \frac{1}{1-s} \right) K_{2/3}(\xi) - \int_\xi^\infty K_{1/3}(t) dt \right], \quad (4)$$

where $\xi = 2s/[3\chi(1-s)]$ and K_n is a modified Bessel function of the second kind. The classical emission rate is obtained by replacing $1-s \rightarrow 1$ wherever it appears. The zeroth moment is the total emission rate $\mathcal{M}(0, \chi) = W_\gamma$. The normalized n th moment is

$$\tilde{\mathcal{M}}(n, \chi) = \frac{\mathcal{M}_q(n, \chi)}{\mathcal{M}_{cl}(n, \chi)}. \quad (5)$$

The subscripts denote whether the quantum or classical emission rates are to be used when evaluating the integrals. For example, the quantum correction to the radiated power [38], sometimes called the *Gaunt factor* [2], is given by $g(\chi) = \tilde{\mathcal{M}}(1, \chi)$. Similarly, the function that controls variance growth due to stochasticity [32] is given by $g_2(\chi) = \tilde{\mathcal{M}}(2, \chi)$.

The classical moments can be evaluated directly:

$$\mathcal{M}_{cl}(n, \chi) = \frac{3^n \sqrt{3} \Gamma(\frac{n}{2} + \frac{1}{6}) \Gamma(\frac{n}{2} + \frac{11}{6})}{2\pi(n+1)} \alpha m \chi^{2n+1}, \quad (6)$$

where the Γ function is defined by $\Gamma(z) = \int_0^\infty t^{z-1} e^{-t} dt$.

The quantum moments cannot be expressed in closed form, so it is more convenient to quote their normalized values. The first step is to express $\tilde{\mathcal{M}}$ as a single integral:

because $R_c \propto \hbar^0$ by virtue of the factor of α . If the corrections due to the higher-order moments σ^2 and ζ^3 are subleading with respect to the quantum correction $\propto \chi_0 \hat{\mu}$, we may neglect all terms containing those higher-order moments and solve this perturbatively by introducing $\hat{\mu} = \hat{\mu}^{(0)} + \chi_0 \hat{\mu}^{(1)} +$

TABLE I. Moments of the classical and quantum photon emission rates.

| n | $\mathcal{M}_{cl}(n, \chi)$ | $\tilde{\mathcal{M}}(n, \chi)$ at $\chi \ll 1$ | $\tilde{\mathcal{M}}(n, \chi)$ at $\chi \gg 1$ |
|-----|---|--|---|
| 0 | $\frac{5}{2\sqrt{3}} \alpha m \chi$ | $1 - \frac{8}{5\sqrt{3}} \chi + \frac{7}{2} \chi^2$ | $\frac{28\Gamma(2/3)}{3^{5/6} 15} \chi^{-1/3}$ |
| 1 | $\frac{2}{3} \alpha m \chi^3$ | $1 - \frac{55\sqrt{3}}{16} \chi + 48 \chi^2$ | $\frac{128\pi}{3^{5/6} 243\Gamma(7/3)} \chi^{-4/3}$ |
| 2 | $\frac{55}{24\sqrt{3}} \alpha m \chi^5$ | $1 - \frac{448\sqrt{3}}{55} \chi + \frac{777}{4} \chi^2$ | $\frac{236\Gamma(5/3)}{3^{5/6} 495} \chi^{-7/3}$ |

$O(\chi_0^2)$. The result is

$$\hat{\mu}(\phi) = \frac{1}{1 + \frac{2}{3}R_c I(\phi)} + \frac{55\chi_0}{8\sqrt{3}[1 + \frac{2}{3}R_c I(\phi)]^2} \int_{-\infty}^{\phi} \frac{R_c |f(\psi)|^3}{1 + \frac{2}{3}R_c I(\psi)} d\psi, \quad (11)$$

where $I(\phi) = \int_{-\infty}^{\phi} |f(\psi)|^2 d\psi$. The first term is the classical result, where the total energy loss depends on the integrated flux [19]. The second term is positive, indicating that the total radiated energy is reduced [38].

A comparison of Eq. (11) with the results of numerical simulations, performed with the Monte-Carlo particle-tracking code PTARMIGAN v1.3.2 [39,40], is given in Fig. 1. In these simulations an electron beam with a mean energy of 500, 1000, or 2000 MeV (Gaussian energy distribution, with 10% energy spread) collides with a plane-wave laser pulse with a Gaussian temporal envelope, normalized amplitude a_0 , a wavelength of 0.8 μm , and a full width at half maximum (FWHM) duration of 30 fs. We vary a_0 in the range $2 < a_0 < 200$ and use either a quantum (stochastic) model of radiation reaction, which builds on photon emission rates calculated in the locally constant field approximation (LCFA) [28,38], or a classical model, which uses the Landau-Lifshitz equation [18]. One may see that the agreement is rather good across the full range of parameters, even though χ_0 is not necessarily much smaller than unity. This may be explained by the fact that our results are first order in χ_0 , but ‘‘all order’’ in the radiation-reaction parameter R_c : as the electron beam loses energy, its instantaneous quantum parameter is reduced and so too the importance of quantum corrections (see Ref. [41] for a similar result).

It may be seen, however, that the theory generally underestimates the energy loss in the quantum case. This is particularly visible for $E_0 = 2000$ MeV around $a_0 \simeq 15$. We explain this by referring the reader to the neglect of higher-order moments in Eq. (10). If the electron energy distribution is very broad ($\sigma \sim \mu$), the first term, which describes energy loss, is increased in magnitude. This is not generally significant under classical radiation reaction, because the variance only ever decreases. Under quantum radiation reaction, by contrast, stochastic effects make it possible for an initially monoenergetic electron beam to develop a broad energy spread. It is reasonable to expect that the error made by Eq. (11) is largest for those collision parameters where the energy spread midway through the laser pulse is largest. We turn, therefore, to the solution of Eq. (2), which describes how the variance of the energy distribution evolves.

IV. BROADENING AND NARROWING OF THE ENERGY SPECTRUM

Expanding Eq. (2) to first order in χ_0 , and neglecting moments of order higher than σ^2 for brevity, yields an equation of motion for the normalized variance $\hat{\sigma} = \sigma/\mu_0$:

$$\frac{d\hat{\sigma}^2}{d\phi} = -\frac{8}{3}R_c |f(\phi)|^2 \hat{\mu} \hat{\sigma}^2 + \frac{55\sqrt{3}}{4}R_c \chi_0 |f(\phi)|^3 \hat{\mu}^2 \hat{\sigma}^2 + \frac{55}{4\sqrt{3}}R_c \chi_0 |f(\phi)|^3 \hat{\mu}^2 \left(\hat{\sigma}^2 + \frac{\hat{\mu}^2}{6} \right). \quad (12)$$

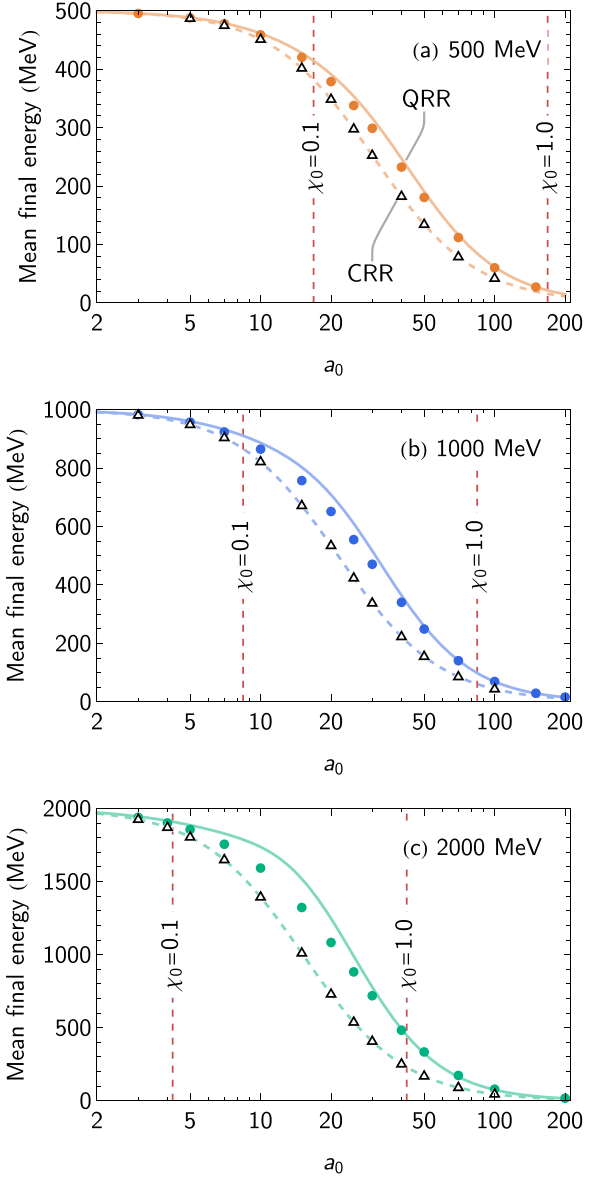


FIG. 1. The mean final energy from simulations (points) and as predicted by Eq. (11), for quantum (solid) and classical (dashed) radiation reactions. The electron beam is initialized with a mean energy of (a) 500 MeV, (b) 1000 MeV, or (c) 2000 MeV. The laser pulse has a normalized amplitude of a_0 , a wavelength of 0.8 μm , and a FWHM duration of 30 fs.

In the classical limit $\chi_0 \rightarrow 0$, we have

$$\hat{\sigma}_{\text{cl}}^2(\phi) = \frac{\hat{\sigma}_0^2}{\left[1 + \frac{2}{3}R_c I(\phi)\right]^4}, \quad (13)$$

which can be expressed as $\sigma/\sigma_0 = (\mu/\mu_0)^2$ in agreement with Neitz and Di Piazza [13] and Vranic *et al.* [34]. This could, in principle, be corrected for nonzero χ_0 in much the same way as done for the mean energy loss, by expanding $\hat{\sigma}^2 = \hat{\sigma}_0^2 + \chi_0 \hat{\sigma}_1^2$, where $\hat{\sigma}_0^2$ is the classical result in Eq. (13). However, the quantum terms in Eq. (12) are not necessarily small corrections to the classical terms. Consider an initially monoenergetic beam, with $\hat{\sigma} = 0$: the leading-order

term in this scenario is the purely quantum term $\propto \hat{\mu}^4$, which drives growth of the variance. The first and second terms, which represent the reduction in the variance due to (quantum-corrected) radiation losses, do not dominate until $\hat{\sigma}$ has grown to a sufficiently large value.

Therefore, we introduce a new parameter V , defined by $\hat{\sigma}^2 = \chi_0 V$, before perturbatively expanding in χ_0 , i.e., $V = V^{(0)} + \chi_0 V^{(1)}$. The equation of motion for $V^{(0)}$ contains the first and last terms of Eq. (12), the competing growth and suppression, at the same order, as desired. Solving this, and then writing $\hat{\sigma}^2 = \chi_0 V^{(0)}$, we obtain

$$\hat{\sigma}_q^2(\phi) = \frac{1}{\left[1 + \frac{2}{3}R_c I(\phi)\right]^4} \left(\hat{\sigma}_0^2 + \frac{55R_c \chi_0}{24\sqrt{3}} \int_{-\infty}^{\phi} |f(\psi)|^3 d\psi \right). \quad (14)$$

One can identify two regimes of behavior in Eq. (14): in the first, the initial variance is sufficiently large that the stochastically driven growth is a small correction; and in the second, the radiation-loss-driven reduction in the variance is a small correction to the growth. Niel *et al.* [33] refer to these as the *cooling* and *heating* regimes, respectively.

We now compare this prediction to the results of numerical simulations. Here we consider the case of quantum radiation reaction and investigate the role of the initial variance σ_0^2 . The electron beam is initialized with a Gaussian energy distribution, with a mean of 500, 1000, or 2000 MeV and a spread (defined by the FWHM) of either 10% or 50% of the mean. As before, the laser pulse is a plane wave with a Gaussian temporal envelope, normalized amplitude a_0 , a wavelength of 0.8 μm , and a FWHM duration of 30 fs. Our results are given in Fig. 2. The qualitative agreement between the theory (solid lines) and simulation results (points) is reasonably good. We see that if the initial energy spread is small, stochasticity drives broadening of the spectrum that is maximized at a particular a_0 . However, if the a_0 is increased beyond this point, radiative cooling dominates and the energy spread is reduced. If, on the other hand, the initial energy spread is large, no stochastic broadening is visible.

The quantitative agreement is not as good as that found for the mean energy, because the contribution of higher-order moments is generally more important for the evolution of σ^2 . (Stochastic broadening leads to increases in both the variance and the skewness, see, for example, Ref. [33].) However, this may be improved significantly by scaling $a_0 \rightarrow a_0/\sqrt{2}$ in Eq. (14). With this correction, shown by the dashed lines in Fig. 2, the agreement is good across the full range of a_0 . The effectiveness of this ad hoc approach may be explained by the fact that it reduces the cooling, which Eq. (12) overestimates because it contains no higher-order moments.

Figure 2 also shows the standard deviation predicted by Eq. (17) in Vranic *et al.* [17], which is derived under the assumptions that the initial energy spread is small and that the laser pulse is long enough that the variance has grown to its maximal value before beginning to shrink. This scaling law is in excellent agreement with our simulation results if a_0 is large, where these assumptions are valid: both our Eq. (16) and Eq. (17) in Ref. [17] predict that $\sigma_f^2 \propto a_0^{-5}$ if $a_0 \gg 1$. It is less accurate for intermediate a_0 , where stochastic broadening and radiative cooling are comparable in magnitude, or if the initial energy spread is large.

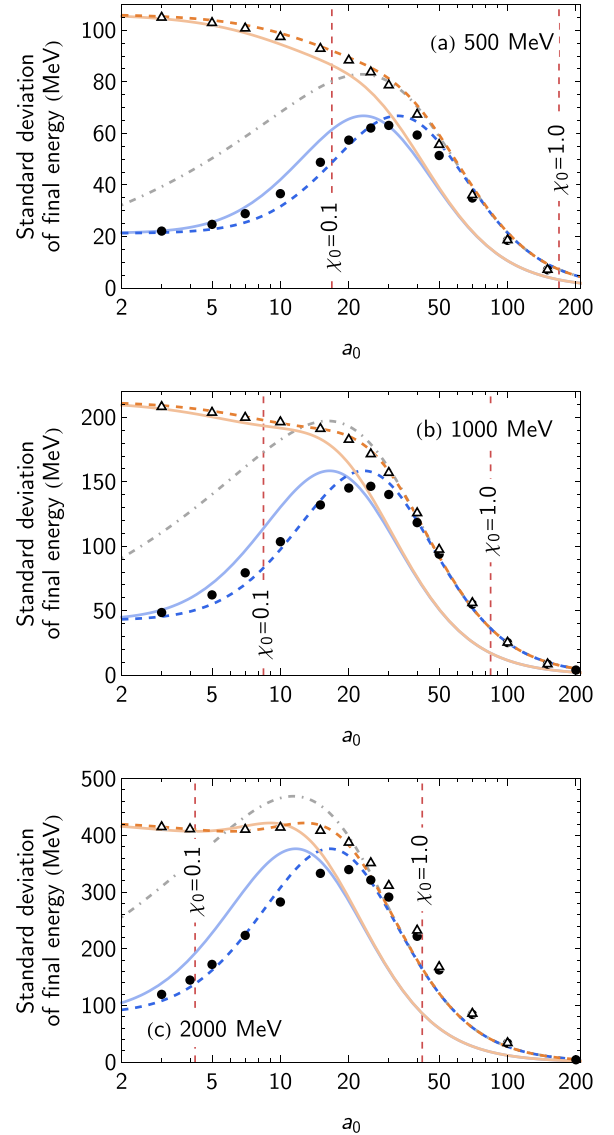


FIG. 2. The standard deviation of the final energy from simulations (points), and as predicted by Eq. (14) (solid lines), for an electron beam with an initial mean energy of (a) 500 MeV, (b) 1000 MeV, or (c) 2000 MeV undergoing quantum radiation reaction. Dashed lines give an ad hoc corrected Eq. (14) (see text for details). Gray, dot-dashed lines give Eq. (17) from Vranic *et al.* [17]. The electron beam is initialized with a Gaussian energy distribution, with FWHM equivalent to 10% (solid disks) or 50% (open triangles) of the mean energy. The laser pulse has a normalized amplitude of a_0 , a wavelength of 0.8 μm , and a FWHM duration of 30 fs.

V. DISCUSSION

Here we present Eqs. (11) and (14) in a more practical form. We consider the case of a linearly polarized laser pulse with a Gaussian temporal envelope, for which $f(\phi) = e_x \sin \phi \exp(-2 \ln 2 \phi^2 / \tau^2)$. Assuming further that the phase duration $\tau \gg 2\pi$, we may average over the fast oscillations and obtain $I(\phi) = (\tau/8)\sqrt{\pi/\ln 2} [1 + \text{erf}(2\sqrt{\ln 2} \phi/\tau)]$. The integral in Eq. (11) cannot be performed analytically: however, it may be shown to be a function of the single parameter $R_c \tau$, so we evaluate it numerically for various $R_c \tau$ and find

a suitable fitting function. Under quantum radiation reaction, the final (normalized) mean and variance are

$$\hat{\mu}_f = \frac{1}{1 + 0.355 R_c \tau} \left[1 + \frac{3.969 \chi_0 \mathcal{F}(R_c \tau)}{1 + 0.355 R_c \tau} \right],$$

$$\mathcal{F}(R_c \tau) = \frac{0.369 R_c \tau}{1 + 0.171 (R_c \tau)^{3/5} + 0.0819 R_c \tau}, \quad (15)$$

and

$$\hat{\sigma}_f^2 = \frac{\hat{\sigma}_0^2 + 0.173 \chi_0 R_c \tau}{[1 + 0.178 R_c \tau]^4}, \quad (16)$$

where we have included the the ad hoc correction discussed in Sec. IV. Under classical radiation reaction, we have instead $\hat{\mu}_f = (1 + 0.355 R_c \tau)^{-1}$ and $\hat{\sigma}_f^2 = \hat{\sigma}_0^2 / (1 + 0.355 R_c \tau)^4$. The collision parameters are given by

$$\chi_0 = 0.812 \left(\frac{E_0}{\text{GeV}} \right) \left(\frac{I_0}{10^{22} \text{ W cm}^{-2}} \right)^{1/2},$$

$$\tau = 1.85 \left(\frac{T}{\text{fs}} \right) \left(\frac{\lambda}{\mu\text{m}} \right)^{-1},$$

$$R_c \tau = 0.954 \left(\frac{E_0}{\text{GeV}} \right) \left(\frac{I_0}{10^{22} \text{ W cm}^{-2}} \right) \left(\frac{T}{\text{fs}} \right), \quad (17)$$

where E_0 is the mean initial energy of the electrons, I_0 is the laser intensity, T is the full-width-at-half-maximum duration of the pulse intensity profile, and λ is the laser wavelength.

Let us consider what these results imply about the collision parameters under which stochastic broadening may be expected. We see from Eq. (16) that the ratio of the final and initial standard deviations, σ_f/σ_0 , is a function of two parameters: a scaled quantum parameter $\chi_0 \mu_0^2/\sigma_0^2$ and a duration-weighted radiation-reaction parameter $R_c \tau$. The region in which stochastic broadening overcomes both the initial energy spread and the effect of radiative cooling is indicated in orange in Fig. 3. It is accessed by increasing the quantum parameter and reducing the initial variance. By contrast, an increase in $R_c \tau$ is generally associated with an increase in radiation losses, which eventually reduce the energy spread. Differentiating Eq. (16) with respect to $R_c \tau$ reveals that there is a maximum at positive $R_c \tau$ if $\sigma_0^2 \lesssim 0.25 \chi_0 \mu_0^2$, namely, $\max(\sigma_f^2) \simeq 0.10 \chi_0 \mu_0^2 / [1 - \sigma_0^2 / (\chi_0 \mu_0^2)]^3$. This is in reasonable agreement with the maximum energy spread (the ‘‘turning point’’ [17] or ‘‘threshold variance’’ [33]) calculated by Vranic *et al.* [17] and Niel *et al.* [33].

The competition between these factors means that stochastic broadening is maximized at a particular a_0 [42], which we derive from Eq. (16) under the assumption that the initial variance is small and all other quantities are held constant:

$$a_0^{\text{opt}} \simeq 160 \left(\frac{E_0}{\text{GeV}} \right)^{-1/2} \left(\frac{T}{\text{fs}} \right)^{-1/2} \left(\frac{\lambda}{\mu\text{m}} \right). \quad (18)$$

The value of the standard deviation at the given optimum is

$$\sigma_f = 370 \left(\frac{E_0}{\text{GeV}} \right)^{5/4} \left(\frac{T}{\text{fs}} \right)^{-1/4} \text{ MeV}. \quad (19)$$

These predict that $a_0^{\text{opt}} = \{33, 23, 17\}$ and $\sigma_f = \{67, 160, 380\}$ MeV for initial energies of $\{0.5, 1, 2\}$ GeV, which is consistent with the results shown in Fig. 2. By expressing σ_f/σ_0 as

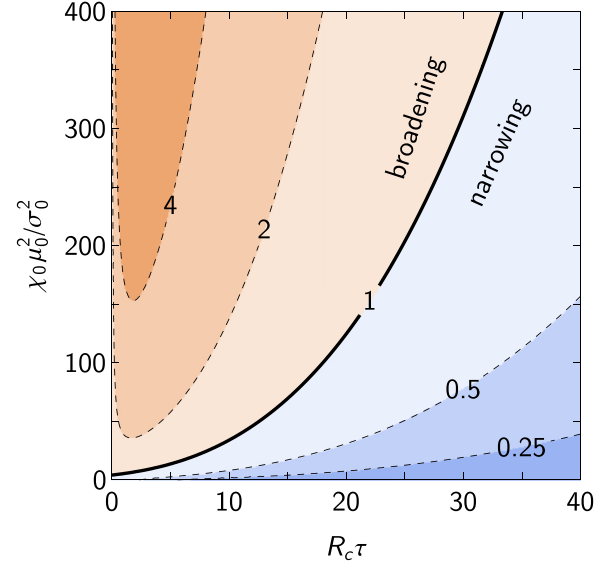


FIG. 3. The ratio of the final and initial standard deviations, σ_f/σ_0 , predicted by the corrected Eq. (16), with broadening ($\sigma_f > \sigma_0$) shown in orange and narrowing ($\sigma_f < \sigma_0$) in blue. Contour lines indicate where σ_f/σ_0 is equal to the labeled value.

a function of $\ln a_0$ and expanding around $\ln a_0^{\text{opt}}$ to second order, we can also estimate the width of this maximum to be $(1/3)a_0^{\text{opt}} \lesssim a_0 \lesssim 3a_0^{\text{opt}}$; this too is consistent with Fig. 2.

It is important to bear in mind that the results in this work have been derived for plane-wave laser pulses. Since the electron beam and the laser pulse in a real experiment are likely to have comparable transverse dimensions ($\sim \mu\text{m}$), finite-size effects are significant. Effectively this means that the different components of the electron beam ‘‘see’’ different peak intensities. The relevant signals are then integrated over a distribution of effective a_0 , dN_e/da , where $0 < a < a_0$: it complicates the identification of quantum radiation reaction effects if the laser pulse and the electron beam have comparable transverse sizes (see analysis in Poder *et al.* [6]). Indeed, broadening of the electron energy distribution would be expected even under classical radiation reaction. The question of whether stochastic broadening is still observable, despite finite-size effects, can be approached directly using three-dimensional (3D) simulations. On the other hand, Amaro and Vranic [43,44] have shown that plane-wave scaling laws, such as those we have here, can be adapted to the fully 3D situation by considering the structure of dN_e/da .

The mean and variance that characterize a beam of electrons are

$$\hat{\mu}_{f,b} = \frac{1}{N_e} \int_0^{a_0} \frac{dN_e}{da} \hat{\mu}_f(a) da, \quad (20)$$

$$\hat{\sigma}_{f,b}^2 = \frac{1}{N_e} \int_0^{a_0} \frac{dN_e}{da} [\hat{\mu}_f^2(a) + \hat{\sigma}_f^2(a)] da - \hat{\mu}_{f,b}^2, \quad (21)$$

where we emphasize that $\hat{\mu}_f$ and $\hat{\sigma}_f$, i.e., Eqs. (15) and (16), are functions of the effective amplitude a . Let us consider an electron beam with spherically symmetric, Gaussian charge density (rms size R) that collides with a focused laser pulse with waist w_0 . Assuming that R is much smaller than the laser Rayleigh range, and that there is no transverse displacement

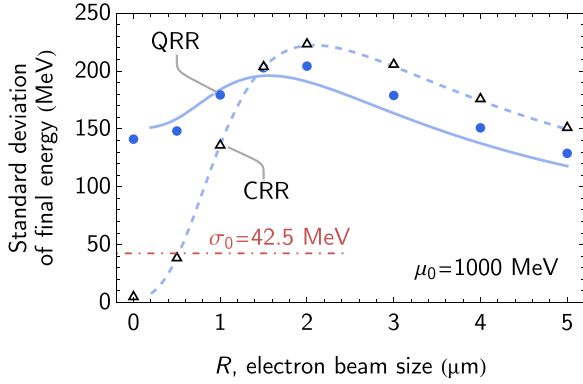


FIG. 4. The final standard deviation in energy of a 1-GeV electron beam (10% energy spread, transverse size R) that collides with a 30-fs laser pulse that is focused to $w_0 = 2.5 \mu\text{m}$ and $a_0 = 30$: from (points) simulations and Eq. (21) for (solid line) quantum and (dashed line) classical radiation reactions.

between the beams, we have [17]

$$\frac{dN_e}{da} = \frac{N_e w_0^2}{aR^2} \exp\left(\frac{w_0^2}{R^2} \ln \frac{a}{a_0}\right). \quad (22)$$

As an example, we compare these 3D-weighted scaling laws with simulations in Fig. 4, for $a_0 = 30$, $w_0 = 2.5 \mu\text{m}$, $\lambda = 0.8 \mu\text{m}$, $T = 30 \text{ fs}$, $\mu_0 = 1000 \text{ MeV}$, and σ_0 equivalent to 10% energy spread. This set of collision parameters is close to the optimum identified in Eq. (18) (see also Fig. 3). We find not only good agreement between the theory and simulations but also that broadening occurs in both the classical and quantum cases. The two can be distinguished, and specifically stochastic effects observed, only if the transverse size of the electron beam is smaller than the laser waist.

VI. SUMMARY

We have presented analytical predictions for the mean and variance of the energy distribution of electron beams that collide with high-intensity laser pulses. This work extends results obtained earlier for classical radiation reaction [13,17,19,34] to the quantum regime. Despite the fact our results are derived assuming that the quantum parameter χ_0 is small, we find that they give accurate predictions for parameters relevant for upcoming experiments, namely, $a_0 < 200$ and initial electron energies in the GeV range. In particular, we are able to show how the initial energy spread of the electron beam affects the possibility to observe stochastic broadening. As it focuses on statistical measures of the electron spectrum, this work will be relevant for upcoming experiments, which will achieve many more collisions at high intensity than were obtained in the first experimental campaigns [5,6].

From our analysis it may be concluded that the best approach to experimental observation of stochastic broadening is to optimize the energy spread and stability of the electron beam, rather than pushing towards higher intensity or electron-beam energy. Increasing the laser intensity in particular is likely to be counterproductive, as it enhances radiative cooling ($R_e \propto a_0^2$) more than it increases the quantum parameter ($\chi \propto a_0$). The scaling laws presented here indicate that a conclusive observation of quantum radiation reaction is well within the capability of current high-intensity laser facilities.

Simulation results were obtained with PTARMIGAN v1.3.2 [40], available from Ref. [39], and may be reproduced using the Supplemental Material [45].

ACKNOWLEDGMENT

The author thanks S. S. Bulanov, C. Riconda, C. P. Ridgers, G. Torgrimsson, and M. Vranic for useful discussions.

- [1] A. Di Piazza, C. Müller, K. Z. Hatsagortsyan, and C. H. Keitel, Extremely high-intensity laser interactions with fundamental quantum systems, *Rev. Mod. Phys.* **84**, 1177 (2012).
- [2] A. Gonoskov, T. G. Blackburn, M. Marklund, and S. S. Bulanov, Charged particle motion and radiation in strong electromagnetic fields, *Rev. Mod. Phys.* **94**, 045001 (2022).
- [3] A. Fedotov, A. Ilderton, F. Karbstein, B. King, D. Seipt, H. Taya, and G. Torgrimsson, Advances in QED with intense background fields, *Phys. Rep.* **1010**, 1 (2023).
- [4] A. Di Piazza, K. Z. Hatsagortsyan, and C. H. Keitel, Quantum radiation reaction effects in multiphoton Compton scattering, *Phys. Rev. Lett.* **105**, 220403 (2010).
- [5] J. M. Cole, K. T. Behm, E. Gerstmayr, T. G. Blackburn, J. C. Wood, C. D. Baird, M. J. Duff, C. Harvey, A. Ilderton, A. S. Joglekar, K. Krushelnick, S. Kuschel, M. Marklund, P. McKenna, C. D. Murphy, K. Poder, C. P. Ridgers, G. M. Samarin, G. Sarri, D. R. Symes *et al.*, Experimental evidence of radiation reaction in the collision of a high-intensity laser pulse with a laser-wakefield accelerated electron beam, *Phys. Rev. X* **8**, 011020 (2018).
- [6] K. Poder, M. Tamburini, G. Sarri, A. Di Piazza, S. Kuschel, C. D. Baird, K. Behm, S. Bohlen, J. M. Cole, D. J. Corvan, M. Duff, E. Gerstmayr, C. H. Keitel, K. Krushelnick, S. P. D. Mangles, P. McKenna, C. D. Murphy, Z. Najmudin, C. P. Ridgers, G. M. Samarin *et al.*, Experimental signatures of the quantum nature of radiation reaction in the field of an ultraintense laser, *Phys. Rev. X* **8**, 031004 (2018).
- [7] S. Weber, S. Bechet, S. Borneis, L. Brabec, M. Bučka, E. Chacon-Golcher, M. Ciappina, M. DeMarco, A. Fajstavr, K. Falk, E.-R. Garcia, J. Grosz, Y.-J. Gu, J.-C. Hernandez, M. Holec, P. Janečka, M. Jantač, M. Jirka, H. Kadlecova, D. Khikhlikha *et al.*, P3: An installation for high-energy density plasma physics and ultra-high intensity laser-matter interaction at ELI-Beamlines, *Matter Radiat. Extremes* **2**, 149 (2017).
- [8] S. Gales, K. A. Tanaka, D. L. Balabanski, F. Negoita, D. Stutman, O. Tesileanu, C. A. Ur, D. Ursescu, I. Andrei, S. Ataman, M. O. Cernaianu, L. D'Alessi, I. Dancus, B. Diaconescu, N. Djourellov, D. Filipescu, P. Ghenuche, D. G. Ghita, C. Matei, K. Seto *et al.*, The extreme light infrastructure-nuclear physics (ELI-NP) facility: New horizons in physics with 10 PW ultra-intense lasers and 20 MeV brilliant gamma beams, *Rep. Prog. Phys.* **81**, 094301 (2018).
- [9] A. Maksimchuk, I. Jovanovic, G. Kalinchenko, C. Kuranz, J. Nees, A. G. R. Thomas, L. Willingale, and K. Krushelnick, Zettawatt-equivalent ultrashort pulse laser system (ZEUS) at the

- University of Michigan, in *Bulletin of the 61st Annual Meeting of the APS Division of Plasma Physics* (2019).
- [10] M. Turner, S. S. Bulanov, C. Benedetti, A. J. Gonsalves, W. P. Leemans, K. Nakamura, J. van Tilborg, C. B. Schroeder, C. G. R. Geddes, and E. Esarey, Strong-field QED experiments using the BELLA PW laser dual beamlines, *Eur. Phys. J. D* **76**, 205 (2022).
- [11] L. Ji, Z. Bu, Y. Wu, X. Geng, B. Shen, and R. Li, Extreme field physics and the 10/100 PW lasers at SIOM, in *Bulletin of the 64th Annual Meeting of the APS Division of Plasma Physics* (2022).
- [12] A. D. Piazza, L. Willingale, and J. D. Zuegel, Multi-petawatt physics prioritization (MP3) workshop report, [arXiv:2211.13187](https://arxiv.org/abs/2211.13187).
- [13] N. Neitz and A. Di Piazza, Stochasticity effects in quantum radiation reaction, *Phys. Rev. Lett.* **111**, 054802 (2013).
- [14] T. G. Blackburn, C. P. Ridgers, J. G. Kirk, and A. R. Bell, Quantum radiation reaction in laser–electron-beam collisions, *Phys. Rev. Lett.* **112**, 015001 (2014).
- [15] C. N. Harvey, A. Gonoskov, A. Ilderton, and M. Marklund, Quantum quenching of radiation losses in short laser pulses, *Phys. Rev. Lett.* **118**, 105004 (2017).
- [16] D. G. Green and C. N. Harvey, Transverse spreading of electrons in high-intensity laser fields, *Phys. Rev. Lett.* **112**, 164801 (2014).
- [17] M. Vranic, T. Grismayer, R. A. Fonseca, and L. O. Silva, Quantum radiation reaction in head-on laser-electron beam interaction, *New J. Phys.* **18**, 073035 (2016).
- [18] L. D. Landau and E. M. Lifshitz, *The Classical Theory of Fields*, The Course of Theoretical Physics, Vol. 2 (Butterworth-Heinemann, Oxford, 1987).
- [19] A. Di Piazza, Exact solution of the Landau-Lifshitz equation in a plane wave, *Lett. Math. Phys.* **83**, 305 (2008).
- [20] H. Heintzmann and M. Grewing, Acceleration of charged particles and radiation-reaction in strong plane and spherical waves, *Z. Phys.* **251**, 77 (1972).
- [21] Y. Hadad, L. Labun, J. Rafelski, N. Elkina, C. Klier, and H. Ruhl, Effects of radiation reaction in relativistic laser acceleration, *Phys. Rev. D* **82**, 096012 (2010).
- [22] C. Harvey, T. Heinzl, and M. Marklund, Symmetry breaking from radiation reaction in ultra-intense laser fields, *Phys. Rev. D* **84**, 116005 (2011).
- [23] T. N. Wistisen, A. Di Piazza, H. V. Knudsen, and U. I. Uggerhøj, Experimental evidence of quantum radiation reaction in aligned crystals, *Nat. Commun.* **9**, 795 (2018).
- [24] C. F. Nielsen, J. B. Justesen, A. H. Sørensen, U. I. Uggerhøj, and R. Holtzapple (CERN NA63 Collaboration), Radiation reaction near the classical limit in aligned crystals, *Phys. Rev. D* **102**, 052004 (2020).
- [25] A. Di Piazza, T. N. Wistisen, and U. I. Uggerhøj, Investigation of classical radiation reaction with aligned crystals, *Phys. Lett. B* **765**, 1 (2017).
- [26] M. K. Khokonov, On the quantum interpretation of the classical schott term in the theory of radiation damping, *Phys. Lett. B* **791**, 281 (2019).
- [27] V. N. Baier and V. M. Katkov, Processes involved in the motion of high energy particles in a magnetic field, *Sov. Phys. JETP* **26**, 854 (1968).
- [28] V. I. Ritus, Quantum effects of the interaction of elementary particles with an intense electromagnetic field, *J. Sov. Laser Res.* **6**, 497 (1985).
- [29] V. Dinu, C. Harvey, A. Ilderton, M. Marklund, and G. Torgrimsson, Quantum radiation reaction: From interference to incoherence, *Phys. Rev. Lett.* **116**, 044801 (2016).
- [30] A. Di Piazza, M. Tamburini, S. Meuren, and C. H. Keitel, Implementing nonlinear Compton scattering beyond the local-constant-field approximation, *Phys. Rev. A* **98**, 012134 (2018).
- [31] T. G. Blackburn, D. Seipt, S. S. Bulanov, and M. Marklund, Benchmarking semiclassical approaches to strong-field QED: Nonlinear Compton scattering in intense laser pulses, *Phys. Plasmas* **25**, 083108 (2018).
- [32] C. P. Ridgers, T. G. Blackburn, D. Del Sorbo, L. E. Bradley, C. Slade-Lowther, C. D. Baird, S. P. D. Mangles, P. McKenna, M. Marklund, C. D. Murphy, and A. G. R. Thomas, Signatures of quantum effects on radiation reaction in laser–electron-beam collisions, *J. Plasma Phys.* **83**, 715830502 (2017).
- [33] F. Niel, C. Riconda, F. Amiranoff, R. Ducloux, and M. Grech, From quantum to classical modeling of radiation reaction: A focus on stochasticity effects, *Phys. Rev. E* **97**, 043209 (2018).
- [34] M. Vranic, J. L. Martins, J. Vieira, R. A. Fonseca, and L. O. Silva, All-optical radiation reaction at 10^{21} W/cm², *Phys. Rev. Lett.* **113**, 134801 (2014).
- [35] S. V. Bulanov, G. M. Grittani, R. Shaisultanov, T. Z. Esirkepov, C. P. Ridgers, S. S. Bulanov, B. K. Russell, and A. G. R. Thomas, On the energy spectrum evolution of electrons undergoing radiation cooling, *Fund. Plasma Phys.* **9**, 100036 (2024).
- [36] G. Torgrimsson, Resummation of quantum radiation reaction in plane waves, *Phys. Rev. Lett.* **127**, 111602 (2021).
- [37] G. Torgrimsson, Quantum radiation reaction spectrum of electrons in plane waves, [arXiv:2310.09863](https://arxiv.org/abs/2310.09863).
- [38] T. Erber, High-energy electromagnetic conversion processes in intense magnetic fields, *Rev. Mod. Phys.* **38**, 626 (1966).
- [39] T. G. Blackburn, PTARMIGAN: Version 1.3.2 (2023), available at <https://doi.org/10.5281/zenodo.7974876>.
- [40] T. G. Blackburn, B. King, and S. Tang, Simulations of laser-driven strong-field QED with Ptarmigan: Resolving wavelength-scale interference and γ -ray polarization, *Phys. Plasmas* **30**, 093903 (2023).
- [41] S. V. Popruzhenko, T. V. Liseykina, and A. Macchi, Efficiency of radiation friction losses in laser-driven ‘hole boring’ of dense targets, *New J. Phys.* **21**, 033009 (2019).
- [42] C. Arran, J. M. Cole, E. Gerstmayr, T. G. Blackburn, S. P. D. Mangles, and C. P. Ridgers, Optimal parameters for radiation reaction experiments, *Plasma Phys. Control. Fusion* **61**, 074009 (2019).
- [43] Ó. Amaro and M. Vranic, Optimal laser focusing for positron production in laser–electron scattering, *New J. Phys.* **23**, 115001 (2021).
- [44] Ó. Amaro and M. Vranic, QScatter: Numerical framework for fast prediction of particle distributions in electron-laser scattering, [arXiv:2308.09348](https://arxiv.org/abs/2308.09348).
- [45] See Supplemental Material at <http://link.aps.org/supplemental/10.1103/PhysRevA.109.022234> for the input files needed to reproduce the simulation results.